Hindawi
Advances in Mathematical Physics
Volume 2021, Article ID 1545098, 13 pages
https://doi.org/10.1155/2021/1545098

Research Article

Feature Extraction and Recognition of Medical CT Images Based on Mumford-Shah Model

Lumin Fan,[1] **Lingli Shen**,[2] **and Xinghua Zuo**[1]

[1]*Medical Equipment Department, Shanghai East Hospital, Shanghai 200120, China*
[2]*Materials Procurement Department, Shanghai East Hospital, Shanghai 200120, China*

Correspondence should be addressed to Lumin Fan; 20150108@stu.nmu.edu.cn

Received 24 August 2021; Accepted 7 September 2021; Published 24 September 2021

Academic Editor: Miaochao Chen

In this paper, we propose an improved algorithm based on the active contour model Mumford-Shah model for CT images, which is the subject of this study. After analyzing the classical Mumford-Shah model and related improvement algorithms, we found that most of the improvement algorithms start from the initialization strategy of the model and the minimum value solution of the energy generalization function, so we will also improve the classical Mumford-Shah model from these two perspectives. For the initialization strategy of the Mumford-Shah model, we propose to first reduce the dimensionality of the image data by the PCA principal component analysis method, and for the reduced image feature vector, we use K-means, a general clustering method, as the initial position algorithm of the segmentation curve. For the image data that have completed the above two preprocessing processes, we then use the Mumford-Shah model for image segmentation. The Mumford-Shah curve evolution model solves the image segmentation by finding the minimum of the energy generalization of its model to obtain the optimal result of image segmentation, so for solving the minimum of the Mumford-Shah model, we first optimize the discrete problem of the energy generalization of the model by the convex relaxation technique and then use the Chambolle-Pock pairwise algorithm We then use the Chambolle-Pock dual algorithm to solve the optimization problem of the model after convex relaxation and finally obtain the image segmentation results. Finally, a comparison with the existing model through many numerical experiments shows that the model proposed in this paper calculates the texture image segmentation with high accuracy and good edge retention. Although the work in this paper is aimed at two-phase image segmentation, it can be easily extended to multiphase segmentation problems.

1. Introduction

In image research and related application development, people usually are not concerned with all the information of the whole image. The object of study is only some local areas in the image, such as image edges and image noise. This local information can be built on a two-dimensional plane or a surface in three-dimensional space. To better identify and analyze local information, we need to separate and extract this information from the image, so that the extracted target can be processed more efficiently and at a deeper level, and it is based on this that the technique of image segmentation was born. In computer digital image processing, image segmentation is a key link [1, 2]. It is the basis of many studies on image processing and analysis, video processing, etc. In computerized digital image processing, image segmentation is a very important subfield. Image segmentation is one of the most extensively studied by many researchers in computerized visual wide subattack. We need to separate and extract this information from the image to process the extracted target more efficiently and deeper. It is based on this that the technology of image segmentation was born. Using this technique, important information can be extracted from images, which can provide very useful material for many fields of image science, while image segmentation techniques are also widely used in daily life [3, 4]. Over the years, several researchers have proposed from a mathematical point of view that the information in an image can usually be viewed as a set of connected regions consisting of a collection of regions, each with its basic features such as edges, image

intensity/color, prior shape, and texture. The goal of image segmentation is to divide an image into specific regions that are adjacent to each other and do not overlap with each other according to different features of the image and to divide these specific regions into different classes, with regions with the same or similar features grouped into the same class and different basic features between classes, which is an important step to achieve content analysis and image understanding [5].

Although the image segmentation problem has been researched and has significantly progressed for more than three decades since it was proposed, no segmentation model can perfectly segment all image types because of the variety of images [6–8]. The active contour model-based segmentation, however, has been widely used in image segmentation and computer vision in the last two decades because it unifies different aspects of image data, target contour extraction, prior knowledge of the image, curve motion tracking, and image reconstruction in one model [9]. The classical active contour models are the Snake model, Mumford-Shah model, geometric active contour model, geodesic active contour model, and so on. Different from the single feature-based image segmentation algorithms, the active contour model combines the level set-based approach and energy generalization and uses both boundary and region features of the image to segment the image in a curve evolution way. After nearly three decades of research and development, segmentation based on the active contour model has become one of the mainstreams and widely used broad classes of segmentation algorithms in the field of image segmentation [10–12]. Using this technology can extract important information in images, which can provide very useful materials for many fields of image science. At the same time, image segmentation technology is also widely used in daily life. Some researchers propose that the information in images can usually be regarded as a set of connected regions; each region has its own basic characteristics, such as edge, image intensity/color, prior shape, and texture. The graph cut represents an image as a weighted undirected graph, where the vertices in the graph represent the pixels of the image, and if the vertices of the image are connected by edges, it means that their corresponding two pixels are adjacent, and the weights of the edges indicate the similarity between each pair of pixels in grayscale, color, or texture. When the image segmentation is completed, each region represents one subgraph. Optimal segmentation means that the pixel similarity in the subgraphs is maximum and the pixel similarity between subgraphs is minimum. In recent years, it has been increasingly widely used in medical image segmentation because it does not require iteration and can achieve global minimization of certain classes of energy functions. It is easy to extract targets from simple homogeneous backgrounds by the graph cut method, but the method faces a big challenge when it is applied to medical images, such as segmentation of liver parenchyma because abdominal CT images often have severe gray-scale distribution inhomogeneity.

This paper focuses on the segmentation problem of medical CT images. After analyzing the classical Mumford-Shah model and related improvement algorithms, we mainly propose the improvement of the classical Mumford-Shah model in two aspects. Firstly, starting from solving the energy generalized minimization problem of the classical Mumford-Shah model, we use the mathematical model and the calculation method of total variance for the energy generalized function and use the idea of CP pairwise to solve the energy of discrete points. On the other hand, from the limitation of the Mumford-Shah model, we improve its initialization strategy and use the methods of dimensionality reduction and clustering to analyze the image data from the perspective of local feature vector reduction and initialization and iteratively update the model generalization. The classic active contour model, such as the Snake model, Mumford-Shah model, geometric active contour model, and geodesic active contour model, is different from the image segmentation algorithm based on a single feature; the active contour model combines the level set-based method and the energy functional at the same time, using the characteristics of the image boundary and region at the same time, and the image is segmented by way of curve evolution. The above two improved perspectives are combined to segment the CT images, which is the object of our study. After the theoretical analysis, we apply the improved method to the actual image data segmentation and analyze the feasibility and applicability of the improved algorithm from the practical level through experiments to analyze the effectiveness of the image segmentation algorithm. The main idea of this paper is to start from the classical active contour model, the Mumford-Shah model, read the related literature to understand the improvement direction of Mumford-Shah model, and determine the improvement direction of this model; apply the mathematical model to the algorithm and conduct theoretical analysis; and then use the algorithm in the actual image segmentation for experiments. In the experimental analysis, the experimental results are compared with those of similar improved algorithms, so that the improved algorithm can be analyzed and summarized.

2. Current Status of Research

To solve the problem that texture images are difficult to represent, literature [13] generated multiscale vector images by the Gabor transform and wavelet transforms and used the Chan-Vese model for vector image segmentation to achieve texture image segmentation, but the above transform will lead to blurred edges of texture image regions. For this reason, literature [14] used an image decomposition variational model to decompose the image into segmented constant-value structured image components and texture image components, and embedded the image decomposition model into the Chan-Vese model to achieve texture image segmentation; this method is not computationally efficient due to the need to solve multiple partial differential equations for the computation of features in different regions. In recent years, the local binary pattern (LBP) method has achieved good results in texture segmentation, which can effectively extract the texture features in images [15]. Compared with Gabor and wavelet transform filters, the segmentation

results obtained based on the LBP algorithm are better and more computationally efficient, but the segmentation results for images with more complex textures need to be improved. Textures in natural images are often highly complex, random, and irregular, so simply considering the inclusion of color and texture features cannot achieve accurate results [16]. The Gabor filter-based model requires the selection of appropriate image channels to obtain the desired results. Shi et al. proposed the N-Cut (normalized cuts) method, which treats an image as an undirected graph with weights; calculates the similarity, that is, the weights between nodes, using the color and luminance information between pixels; and proposes a normalized criterion for graph cuts which divides the image into two parts: target and background, and this method leads to oversegmentation or undersegmentation [17].

As one of the region-based models, the Mumford-Shah model is the basis of variational image segmentation, and its basic idea is to segment images with segmented smooth images and their boundary approximations; however, the problem is unsolvable due to the inconsistent dimensionality of images and contour lines [18]. To facilitate direct computation, the literature introduced a level set function to divide the region, expressed the segmentation line length in terms of total variation (TV), and transformed the Mumford-Shah model of segmented constant-value degeneracy into the Chan-Vese variational model of integration over the region, and Huang et al. directly adopted the binary labeling function and proposed the Chan-Vese variational model based on the binary labeling function [19]. These variational models are based on the binary labeling function. To describe the texture features in images, Bresson et al. transformed the classical Mumford-Shah model into a nonlocal Mumford-Shah model using nonlocal operators, which provides a good framework for texture image segmentation. This paper is an extended study based on this. Since color texture images contain more texture features and color information, the robustness of the model becomes more demanding, and the operations of multiple channels involved in the color model can lead to blurred texture features and edge information and poor segmentation results when layers are superimposed, which are the problems researchers focus on. The classic active contour model, the Snake model, Mumford-Shah model, geometric active contour model, geodesic active contour model, etc., is different from the image segmentation algorithm based on a single feature; the active contour model combines the level set-based method and the energy functional at the same time, using the characteristics of the image boundary and region at the same time; the image is segmented by the way of curve evolution. Dehkordi proposed a way to view the image as a set consisting of level set curves, and the evolution curves are implicitly represented as 0-valued mapping methods of high-dimensional functions [20]. To determine the target boundary, this method deals with the problems present in the topology of the zero-level set of curves by controlling the evolution of the zero-level set curves. Hasan gave a nonparametric model of the geometric activity profile by embedding the evolution curve of the model in the level set equation [21]. The idea is to use image information and continuous curves to define the problem-specific energy generalization and image edges, respectively, by solving the Euler-Lagrange equation from the variational principle to obtain the corresponding equation [22]. By solving the Euler-Lagrange equation by the variational principle, the corresponding curve evolution equation is obtained, and then, the gradient flow equation about the level set function is introduced, and the optimal segmentation closed contour line can be obtained by numerically solving this equation. The ability to solve the problems of the parametric active contour model is the main advantage of this model.

Although deep learning produces a great boost in the analysis and diagnosis of some important diseases, it is still difficult to deal with complex global lesions and structural lesions with complicated clinical needs, and many medical imaging problems will not be solved in a short time, such as CT images of a brain hemorrhage. This is because methods such as deep learning are limited by the quality and quantity of samples and the effectiveness of algorithms, inadequately solving the problem, and the accuracy and efficiency need to be further improved. To study and optimize the core algorithm and structure of brain hemorrhage CT images, and to make the model more accurate, fast, and effective in analyzing medical images, the necessary means and steps of "AI+medical imaging" are required.

3. Mumford-Shah Model for Medical CT Image Feature Extraction and Recognition Analysis

3.1. Improved Mumford-Shah Model. The classical Mumford-Shah model solves the image segmentation problem at the mathematical level by transforming the curve evolution process of image segmentation into the integration of the image segmentation resultant features and the segmentation problem into the minimization problem of solving the model generalized function. In the paper of Mumford and Shah, the energy generalized expression proposed by both Mumford and Shah is

$$E(f,P)=\mu^2\left(\iint_R (f+g)^2 dxdy-\iint_R (f-g)^2 dxdy\right). \quad (1)$$

In solving the Mumford-Shah model, the most widely used method for solving the energy generalized minimum is the level set method [23]. The level set method is explained by the mathematical model that a closed curve in space can be represented as the intersection of a three-dimensional surface and a plane, and a closed curve varying in space can be represented as the level set obtained from the intersection of a cluster of surfaces and a plane that varies with time. This means that the object of study is transformed into a surface evolution problem that tracks the evolution of a higher-order surface, and numerical computation is performed during the evolution iteration. Thus, the model has the characteristics of dynamic change and adaptive topology, and the target set of contour curves is finally obtained after iteration. The pure level set method is to use curve evolution to approximate the idea of image segmentation curve, while

the level set method to solve the Mumford-Shah model is to regard the model as a curve evolution process and convert the energy expression of the curve into a level set function. At present, the level set method has been widely used in 2-dimensional and 3-dimensional spatial images, and compared with other algorithms such as watershed algorithm and threshold method, the level set method is more often used in the medical field. Both the level set method and the Mumford-Shah model algorithm based on the level set method have been widely used for image segmentation in 2-dimensional and 3-dimensional spaces.

While the pure level set approach is the idea of approximating the image segmentation curve by curve evolution, solving the Mumford-Shah model by the level set approach is to view the model as a process of curve evolution, converting the energy expression of the curve into a level set function and solving it in an iterative process. In simple terms, solving the energy generalization function by the level set is simplifying the Mumford-Shah model by the level set algorithm and solving the numerical problem of the energy generalization function further. By the above analysis, the level set function of a closed curve in a two-dimensional image is expressed as follows:

$$\begin{cases} \phi(x_1, x_2, t) < 0, & (x_1, x_2) \text{ inside } C, \\ \phi(x_1, x_2, t) = 0, & (x_1, x_2) \text{ on } C, \\ \phi(x_1, x_2, t) > 0, & (x_1, x_2) \text{ outside } C. \end{cases} \tag{2}$$

In addition to the above-mentioned level set approach, a widely accepted and continuously improved model combining the Mumford-Shah model with the level set approach is the C-V model proposed by Chan and Vese. This reorganizes and simplifies the energy generalization of the M-S model.

$$F(C, c_0, c_b) = \mu L(C) - \nu S_0(C) - (\lambda_0 - 1)\int_{\text{in}} |I + c|^2 dxdy. \tag{3}$$

In the solution process, the C-V model is solved using the level set method, replacing the closed target contour $C(t)$ with the level set function $\varphi(x, y, t)$, which allows obtaining the energy generalization function.

$$E(u^+, u^-, \varphi) = \int_\Omega |u^+ + u^-|^2 H(\varphi) dxdy. \tag{4}$$

In this chapter, we improve the solution of the Mumford-Shah model based on the Mumford-Shah model itself, and we do not introduce the variational solution of the model here. The current algorithms for the numerical approximation of the Mumford-Shah model are mainly divided into the approximation using convex optimization algorithms such as split-Bregman and the solution of the PDE partial differential equation based on the Euler-Lagrange equation [24]. Among the approximation algorithms, the split-Bregman algorithm, as a commonly used convex optimization approximation algorithm, is an iterative computational sequence obtained by combining the original Bregman iteration algorithm with the split algorithm by variable substitution. And the above-mentioned method for solving partial differential equations based on the Euler-Lagrange equation is mainly applied to the algorithm for solving the Mumford-Shah model using level sets and the C-V algorithm based on the Mumford-Shah model, which transforms the energy generalization of the Mumford-Shah model into a solution of the Euler-Lagrange equation according to the variational theorem. However, this equation cannot be solved directly to obtain the minimum value, and the local extrema need to be approximated by the gradient descent method, so the solution process is more complicated and the result may not be the global optimal solution.

$$E = \max \sum_{l=1}^{K} \left\{ \int I_l dx - \lambda \text{Per}(\text{R}_l, R) \right\}, \tag{5}$$

$$\lim_{N \longrightarrow \infty} \sum_{i=1}^{N} \left(\frac{f(x_i - 1) + f(x_i)}{2} \right) > 0. \tag{6}$$

Convex relaxation techniques are used to solve or approximate the optimal solution of a discrete variable or nonconvex function by relaxing it into a convex optimization problem. In simple terms, the original definition domain of a single point set is relaxed to the real number range and the objective function is adjusted, or the nonconvex function is transformed into a convex function so that it is no larger than the original objective function, and then, the convex optimization method can be used. To avoid this limitation, we need to make the adjusted objective function also convex in the definition domain, so that it can be solved numerically by the analytical method directly, and then, it can be rectified. Convex optimization methods are widely used in solving optimal solution problems because the local optimal solution obtained in a convex problem is equivalent to the global optimal solution of the problem. In addition, the Lagrangian dual in convex optimization provides the superiority of the convex optimization algorithm to ensure the validity of its optimal solution. For convex relaxation techniques, the common ones are the Lagrange relaxation algorithm, linear programming relaxation algorithm, and pairwise programming relaxation algorithm, as shown in Figure 1.

For the minimax solution problem of the energy generalization, we first define an extensive solution model.

$$E(A) = \int_\Omega |u^+ + u^-|^2 H(\varphi) dx. \tag{7}$$

In short, without considering the cost of smoothness, then the minimum value problem for the energy like generalized functions is the problem of solving the minimum of (8) as follows:

$$E(A) = \max \int_\Omega |u^+ + u^-|^2 H(\varphi) dx. \tag{8}$$

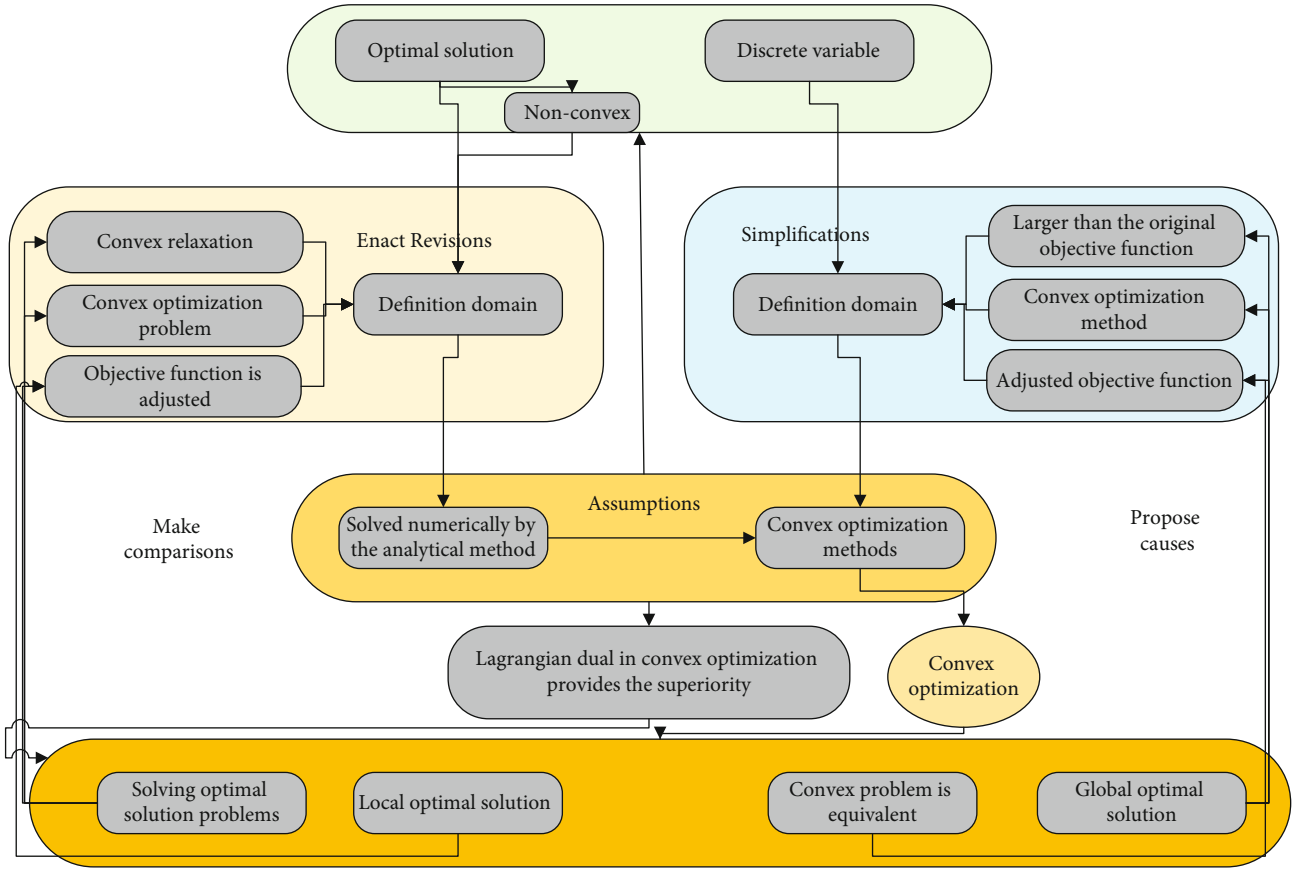

Figure 1: Improved Mumford-Shah model.

Considering the above optimization problem as a linear programming problem, then we can obtain its dual problem as follows:

$$\min \int_{\Omega} |u^{+} + u^{-}|^{2} H(\varphi) dx > 0. \tag{9}$$

Considering that the variables in the energy generalization formula of the model exist mostly in the form of sets, solving the problem directly will be an NP-hard problem. To better find or approximate the optimal solution, we adjust the image feature terms of the model and propose the concept of an indicator function, which considers the fidelity term of the energy generalization function, i.e., the difference integral of the input image and the segmented image, and solves it mainly by adjusting the edge terms by the indicator function. The BV bounded variance and the pairwise idea are mainly used to organize it into the form of the total TV variance, and the model is relaxed into a convex optimization problem using convex relaxation techniques [25]. In the optimization process, there may be a local minimum. To avoid this limitation, we need to make the adjusted objective function convex in the domain, so that we can directly solve the optimization numerically through the analysis method, and finally round it. For the improved convex optimization problem, after reading a series of literature, we decide to use the Chambolle-Pock algorithm to discretize the relaxed TV total variance model and then compute it, mainly for the discretized part of the TV total variance. After theoretical analysis, we give the steps of the Chambolle-Pock algorithm applied to this model.

$$\max \quad \max \left\| F(g)x + F(g)x' \right\| \geq 0, \tag{10}$$

$$\min \quad \max \left\| F(g)x + F(g)x' \right\| > 0. \tag{11}$$

Clustering methods, often called unsupervised learning algorithms, simply mean that the data set is divided into different classes or clusters according to some set criteria, and the data or data features in each class or cluster are as similar as possible, while the differences between different classes or clusters are as large as possible, and the data obtained by clustering often vary greatly for different computational methods or given training sets. So far, clustering algorithms have been widely used in different fields, and the clustering algorithms for high-dimensional data applied in fields such as deep learning, data mining, and statistics are constantly being improved.

The local spectrum histogram is usually performed using a Gabor filter, while other frequently used filters are a Gaussian filter, a Gaussian filter with Laplace operator, or a simple intensity filter. Considering that we will use the proposed local spectrum histogram in its entirety in our experiments,

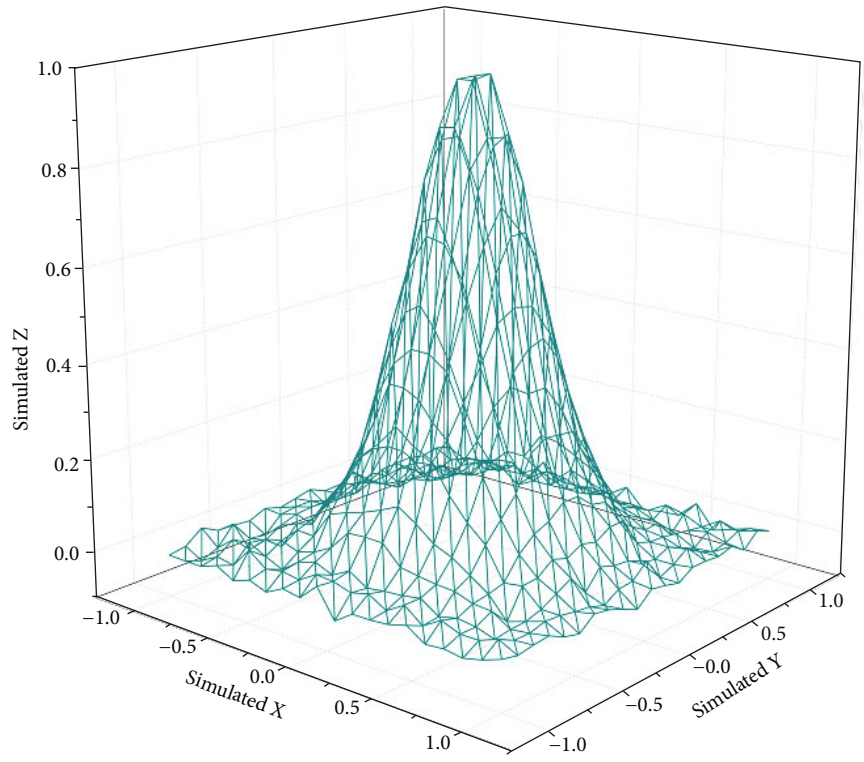

Figure 2: Initial level set function.

we will use the Gabor filter in our experiments. For the application of the local spectral histogram, we first select the Gabor filter to act on the image data, thus producing the filtered image $\{g1, \cdots, gp\}$, from which we can obtain this feature extractor.

$$F_{SH}[g](x) = \frac{\sum_{x_k} \int \delta(z + g_{ik})dz}{W_s(x)}. \tag{12}$$

We use the average features in different structural regions as a feature extractor.

$$c = F(g)x + F(g)x'. \tag{13}$$

In addition to the introduction of the above two mathematical models and the analysis of their theoretical feasibility in the field of image segmentation, we also combine our two proposed improvement perspectives and give detailed steps of the algorithm. We codify the improved algorithm proposed in the above two chapters and apply it to a real image segmentation experiment, thus testing the feasibility of the algorithm and the performance and efficiency of the algorithm from a practical point of view, as shown in Figure 2.

The curve evolution process is represented using the minimization energy generalization function, and the length of the curve is defined by the following generalization function.

$$\max\left\{E(C) = \sum_{s=1}^{n} ds\right\}. \tag{14}$$

Color features best reflect the surface properties of an object or scene contained in an image, and each pixel in an image has its meaning and contribution. Color features not only describe global features but also capture local features in an image, and they are inherently resistant to sensitivity. Although color features have their advantages, they also have their shortcomings. Color features are based on pixel point features, so they cannot cover the relationship information between regional pixels, multiscale information, etc.

$$P(i, j) = (x, y). \tag{15}$$

The active contour model method turns the image segmentation problem into a curve evolution problem. According to the representation and realization of the curve, the active contour model can be divided into the parametric contour active model and the geometric active contour model. In the Lagrangian formulation, the parametric activity contour model expresses the evolution curve explicitly, while the geometric activity contour model represents this evolution curve implicitly utilizing a level set that evolves from the Euler formula. Some methods use a priori knowledge to determine the grayscale range of the liver, which is fast but may lose effectiveness when the grayscale of the target varies unevenly.

3.2. Experimental Design of Medical CT Image Feature Extraction and Recognition. During the acquisition and transmission of CT images of cerebral hemorrhage, noise is often generated along with it. When the attenuation coefficients of normal and pathological tissues are very close, the presence of noise will reduce the signal-to-noise ratio of

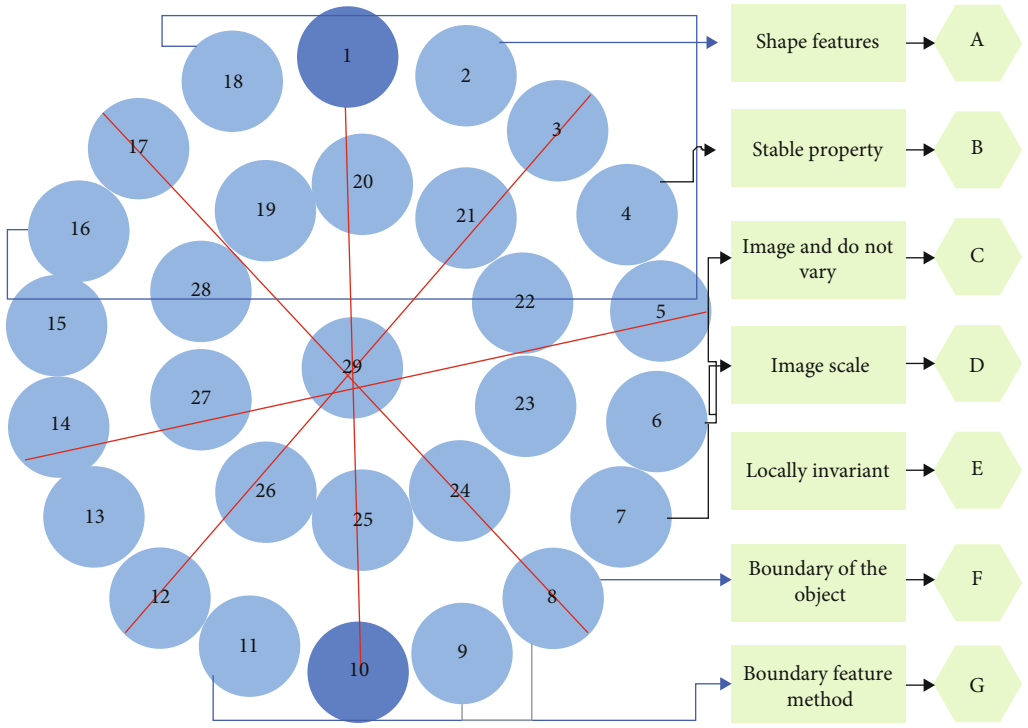

Figure 3: Diagonal diagram.

the image, which will make the details of the edges of the hematoma of cerebral hemorrhage masked by the image noise, so that the segmentation effect of the hematoma is poor, and in serious cases, it will directly affect the doctor's judgment in terms of the disease. From the above problem, we can analyze that removing noise from CT images of cerebral hemorrhage is a basic part of the preprocessing process. For different calculation methods or a given training set, the data obtained through clustering is often very different. So far, clustering algorithms have been widely used in different fields, and clustering algorithms for high-dimensional data used in fields such as deep learning, data mining, and statistics are also constantly being improved. Impulsive noise, Gaussian white noise, and mixed noise are common noises in CT images of a cerebral hemorrhage. Among them, the location of the impulse noise is random, but the amplitude of the noise is unchanged, while the location of the Gaussian white noise is deterministic, and its amplitude is randomly changed [26]. The mixed noise is the noise mixed with impulse noise and Gaussian white noise. In the denoising process, the corresponding denoising algorithm needs to be selected according to the characteristics of the noise, for example, for pepper noise, the median filtering algorithm has better processing results, but for Gaussian noise, the median filtering algorithm is less effective. At this time, the mean filtering algorithm, wavelet algorithm, or Wiener filtering algorithm should be selected, but these algorithms are not suitable for processing pepper noise.

Shape features are a stable property of an image and do not vary with the image scale, brightness, or viewpoint and are locally invariant. Shape features include contour features that focus on the outer boundary of the object and area features that target the entire shape region. The main idea of the boundary feature method is to characterize the boundary features of the image by using some boundary detection methods to obtain the shape parameters with characterization significance. Typical methods are Hough transformation to detect parallel straight-line method and boundary direction histogram method. Transformation is to connect the edge pixels to form a closed region boundary; the boundary direction histogram is usually to construct the gray gradient direction matrix of the image and make a histogram by the obtained image edge, as shown in Figure 3.

Spatial relationship refers to the mutual spatial location information or relative orientation relationship information among multiple segmentation targets in the image. The spatial position information can be divided into two categories: relative spatial position information that emphasizes the relative situation between targets and absolute spatial position information that emphasizes the distance size and orientation between targets. Relative directional relationship refers to connection/adjacency relationship, overlap/overlap relationship, inclusion/inclusion relationship, etc. The spatial relationship features have certain discriminative power but are not rotation invariant as well as scale-invariant to the image. There are two ways to extract the spatial relationship features of an image: the first is to segment the image into multiple regions according to some segmentation algorithm and then extract features in these regions and build indexes; directly segment the image into uniform regular blocks and then extract individual block features and build indexes.

The energy general function-based segmentation method is a hot research topic among existing image segmentation methods, which mainly includes the parametric

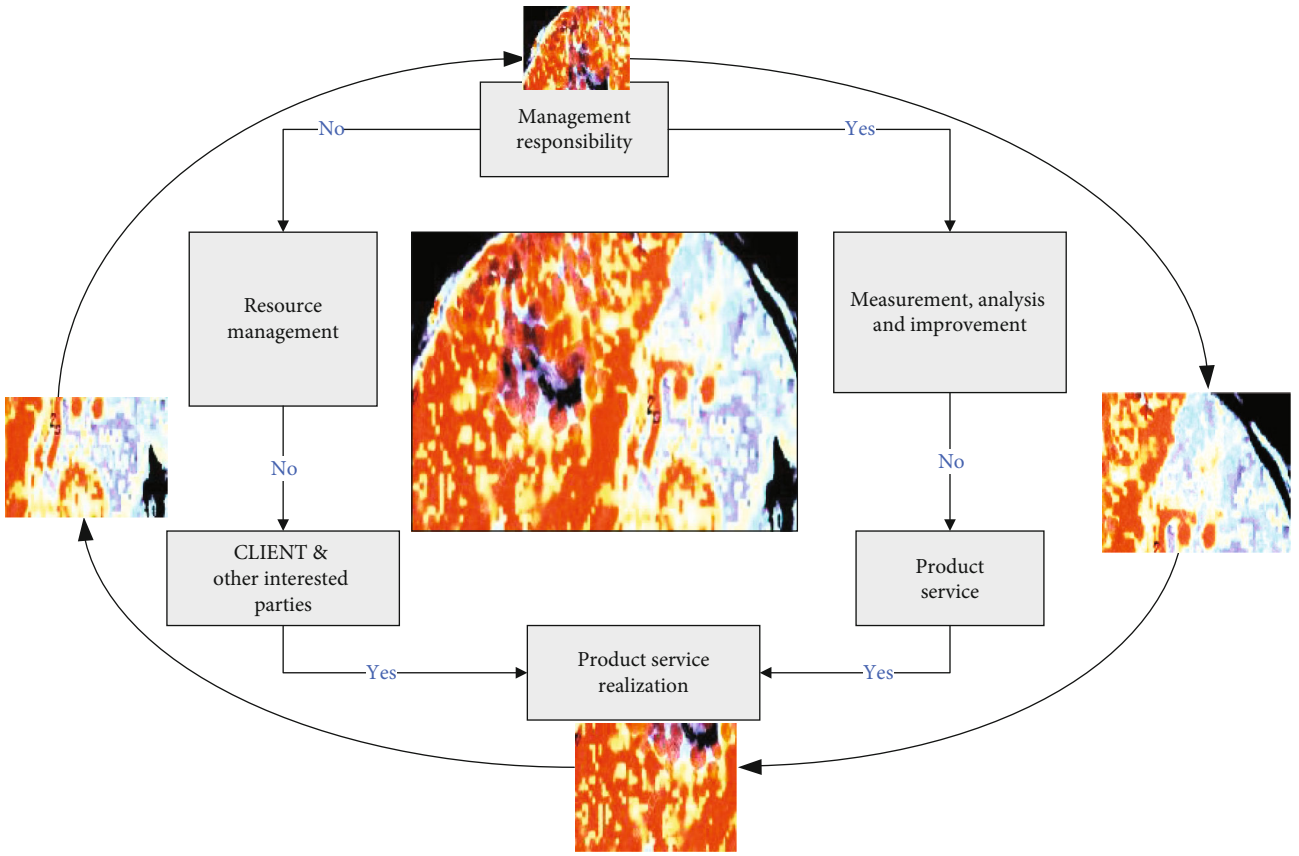

Figure 4: Experimental steps.

active contour model represented by the Snake model and the geometric active contour model based on the level set method; the latter is often called the level set method. The core idea of the level set method is to use a continuous curve to express the target contour and define an energy generalization function so that its independent variables include the curve, transforming the segmentation process into a process of solving for the minimum of the energy generalization function. In the traditional method, the initial point is usually set at the average position of the two lumens of the mapped coronary model to avoid misjudging the lumen position. This is because a consistent definition of the initial point is essential when using the minimum path-based method for path tracking, especially during the extraction of the coronary centerline. However, using this method, using the average position instead of the luminal position introduces a huge position error during the alignment process. So, the model-based directed shortest path coronary centerline extraction algorithm uses a 3D Haar feature-based and probabilistic boosted tree framework to detect the luminal position. This method combines the image intensity information and the information processed by the vessel's algorithm for feature calculation and training, which can improve the accuracy of detection, as shown in Figure 4.

Comparing the above two cases, contour initialization will cause some time wastage; therefore, this paper can replace the process of human initialization with suspected hematoma region detection [23]. However, the hematoma detection mainly revolves around the arbitrary location of the hematoma, the specificity of the hematoma size, and the irregularity of the hematoma shape, and if a rectangular box is used to define the hematoma, the rectangles have different aspect ratios. Since the hematomas have different aspect ratios, it is too costly to solve the hematoma detection problem using the classical sliding window combined with image scaling.

Threshold segmentation is a method that uses the grayscale information of image regions for processing. The idea of threshold segmentation is relatively simple, and the core lies in obtaining the appropriate grayscale threshold to classify each pixel in the image, and the selection of the threshold value becomes exceptionally critical. Usually, the threshold value is determined by the image's grayscale distribution, which can be calculated by specific rules. The method works well especially for images with a wide range of differences in the distribution of background and foreground pixels. In practical applications, the key to using this method is to find the threshold that distinguishes the foreground from the background. To get the correct threshold, the enumeration method is usually used, and thresholds of different sizes are brought into the required operation to derive the intraclass variance of the foreground and background calculated for each threshold, and the required threshold is obtained by ensuring that the intraclass variance is an extreme value.

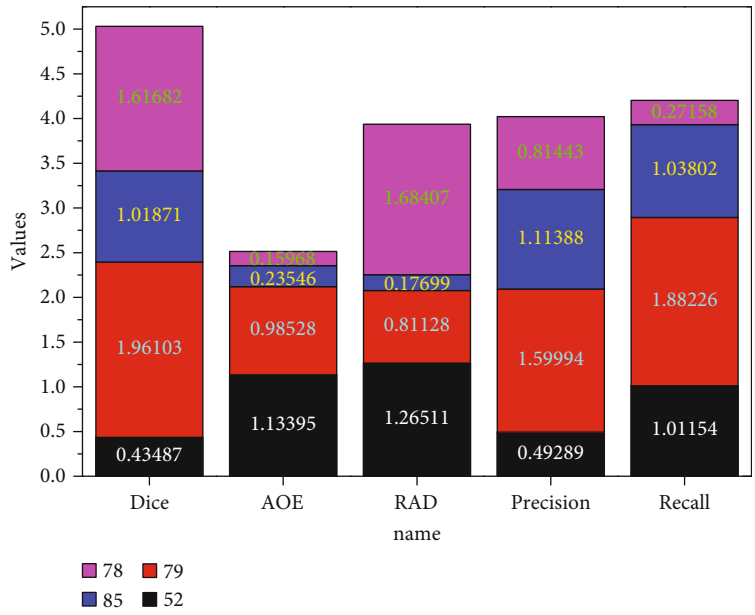

Figure 5: Algorithm performance evaluation table.

4. Analysis of Results

4.1. Mumford-Shah Results. To verify the superiority of the distance regularization level set algorithm that combines region information and edge information, a lot of experiments are done in this paper, and some parameter settings are given below. The time step is 1, the constant peal is set to 5, s is 1.5 and 0.8, and α is -5, and the number of iterations is set differently according to the pictures. The first column shows the original abdominal CT, the second column shows the segmentation result of the algorithm in this paper, and the third column shows the comparison image between the algorithm and the gold standard (red is the segmentation result of the algorithm, green is the segmentation of the gold standard); from Figure 5, we can see that the algorithm and the gold standard only have a small error and can achieve good segmentation results. To further evaluate the segmentation performance of the algorithm, we performed mathematical calculations on the segmentation results and the gold standard segmentation, and the five performance indicators we used are area overlap error, recall, DICE index, relative area difference, and accuracy, and the calculation results are shown. From the figure, we can see that the algorithm in this paper achieves good performance in each of the metrics.

To test the ability of the algorithm in this paper to segment the liver images in abdominal CT with nonuniform grayscale, we compare the distance regularized level set incorporating both region information and edge information with the distance regularized level set driven by only single edge information. To ensure the fairness of the experiments, we repeatedly did several experiments for the improved DRLSE model and the edge-based DRLSE model in this paper and obtained several experimental results, of which we selected the best one to show. The main idea is to set a gray threshold of an isosurface, compare the eight corners of the voxel with the threshold of the is surface, and judge whether the eight corners of the voxel belong to the isosurface. Connect the voxel corner points on the isosurface, to form the surface information in the three-dimensional data field. As shown in the figure, we give the segmentation results of three abdominal CT images; the first column is the original CT image, the second column is the segmentation result of the improved DRLSE, and the third column is the segmentation result of the edge-based DRLSE. From the figure, we can see that the distance regularization level set is driven by only single edge information that results in edge leakage.

In general, the distribution of the gray value of pixel points in an image can be approximated by the Gaussian function. When segmenting a grayscale inhomogeneous image, it is important to choose the appropriate scale parameter o because the grayscale inhomogeneous image varies a lot in different regions. If we say that only one scale o is used for the whole image, then we cannot accurately obtain the local neighborhood feature information of each pixel point, and it is also worth thinking about how to determine this single scale o so that the segmentation effect can be optimal. In this paper, through a multiscale approach, we can obtain different scale parameters for unevenly distributed grayscale images with different segmentation regions, as shown in Figure 6.

Face drawing refers to the rendering and smoothing operations performed directly on the equivalent faces to obtain a 3D model of the object. An equivalent surface is a collection of points with the same value. The most used method in face drawing is the Marching Cube method. The main idea of the Marching Cube (MC) method is to set a grayscale threshold of the equivalence surface, compare the eight corner points of the voxel with the threshold of the equivalence surface, and determine whether the eight corner points of the voxel belong to the equivalence surface. The

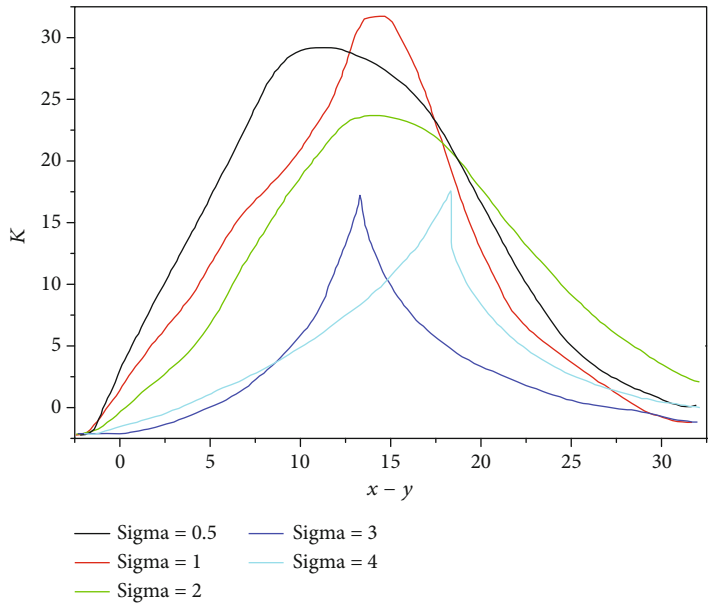

Figure 6: Gaussian curve response graph.

voxel corner points located on the equivalence surface are connected so that they constitute the surface information in the 3D data field. Body drawing is the processing object of the voxel, through the opacity value and color value of the voxel to directly express the target object, and the voxel is a cubic area composed of eight adjacent sampling points. Among the many-body drawing methods such as light and shadow projection and snowballing, the most used method is still the light and shadow projection method, because the light and shadow projection method is in line with the human eye's perception of object imaging and can also achieve a good degree of accuracy. Although the body drawing algorithm has a shortage of large computation, with the maturity of the corresponding hardware technology of image processing, this method will become the mainstream algorithm of future 3D reconstruction.

4.2. Medical CT Image Feature Recognition Results. To filter out the image features with statistical significance and strong diagnostic ability, feature optimization is performed by calculating the evaluation index P value and AUC value and reducing the dimensionality of the feature vector. When $P < 0.05$, it indicates that the features are statistically significant; when $AUC > 0.5$, it indicates that the features have diagnostic significance. Based on this, the features that satisfy both the asymptotic significance $P < 0.05$ and $AUC > 0.6$ conditions are selected to form the final feature vector as the input of the classification model, which is used to study the classification of positive abnormalities in liver plain CT images. Because of the large number of feature extraction methods used, many features were obtained, and only some of the features that satisfy the requirements of P and AUC values are selected and shown in Figure 7.

The liver CT images were processed by traditional feature extraction methods; the features such as grayscale coeval matrix (GLCM), grayscale gradient coeval matrix (GGCM), local binary patterns (LBP), and shape invariant moments (HU Invariant Moments) were extracted; the optimal feature set was selected as the input of the classifier according to the asymptotic significance P value and AUC value; the classification accuracy was evaluated by the evaluation indexes SEN, SPE, PPV, NPV, and ACC which were used to evaluate the performance; the classification accuracy of positive abnormalities of liver CT images was finally obtained; and the specific experimental results are shown in Figure 8.

Analyzing the data in Figure 8, it can be concluded that the features extracted by the single methods of GLCM, GGCM, LBP, and HU invariant moments have some ability to characterize the image information, but the accuracy is lower than the accuracy after the fusion of the four methods because of the single feature description. Compared with the least effective shape invariant moment method, SEN, SPE, PPV, NPV, and ACC improved by 10%, 15.1%, 10.8%, 14%, and 12.2%, respectively. Compared with the best experimental LBP method, SEN, SPE, PPV, NPV, and ACC were improved by 2.5%, 3.8%, 2.7%, 3.5%, and 3.1%, respectively. The fused features have not only the grayscale information gradient information of the image but also the local feature information as well as the shape and contour information of the image, which makes the feature description more comprehensive, and the accuracy rate is significantly improved. The accuracy rate is lower than the accuracy rate after the fusion of the four methods. Compared with the worst experimental shape invariant moment method, SEN, SPE, PPV, NPV, and ACC improved by 10%, 15.1%, 10.8%, 14%, and 12.2%, respectively. Compared with the best experimental LBP method, SEN, SPE, PPV, NPV, and ACC were improved by 2.5%, 3.8%, 2.7%, 3.5%, and 3.1%, respectively. The fused features have not only the grayscale information gradient information of the image but also the local feature information as well as shape and contour

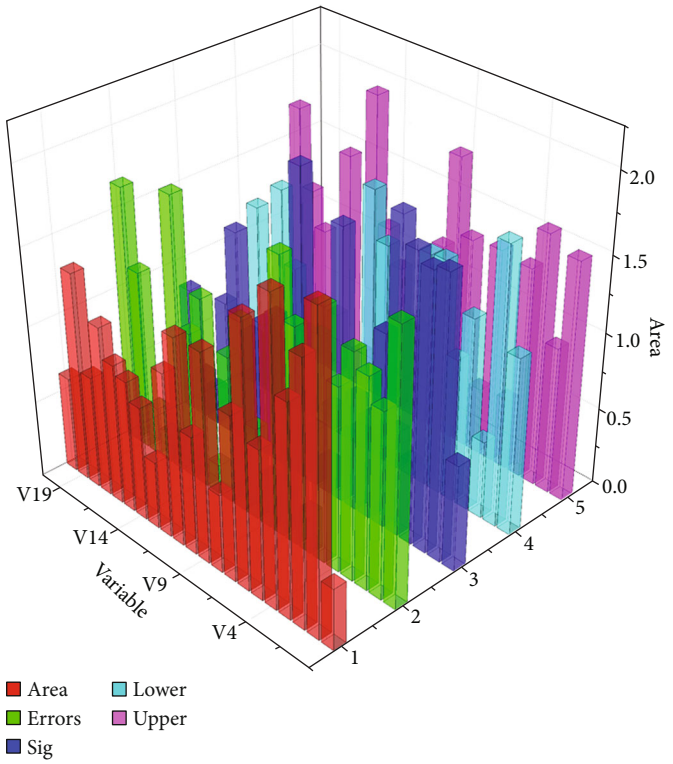

Figure 7: Area under the curve test result variable.

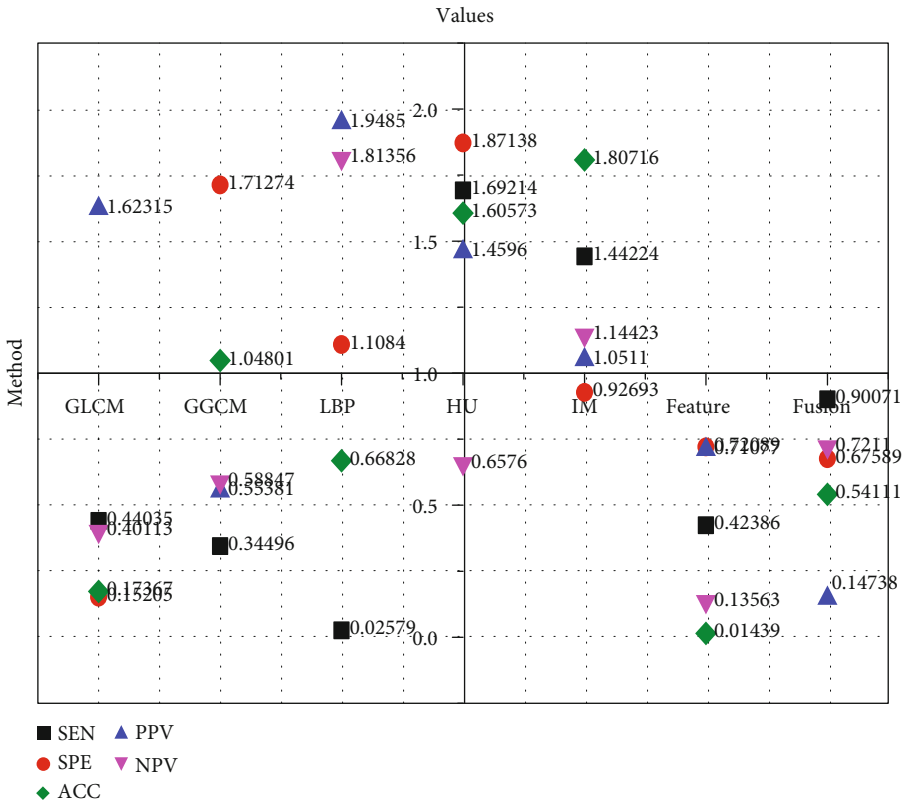

Figure 8: Experimental results.

information of the image, which makes the feature description more comprehensive, and the accuracy rate is significantly improved. The main idea is to set a gray threshold of an isosurface, compare the eight corners of the voxel with the threshold of the isosurface, and judge whether the eight corners of the voxel belong to the isosurface. We connect the voxel corner points on the isosurface to form the surface information in the three-dimensional data field.

The depth features obtained by SE-ResNeXt were fused with the high-quality features obtained by traditional methods and logistic regression analysis, and the final accuracy reached 97.65%, which improved 1.25% compared with the accuracy of fusion between traditional features and 0.35% compared with the accuracy of depth features alone, so according to the results of several experiments, the proposed multifeature fusion liver CT image feature extraction method based on deep learning is verified to have certain advantages and feasibility.

By using deep learning to train the images to obtain high-level semantic features and fusing them with the features with high discriminative power obtained by the traditional algorithm, a feature vector that can comprehensively describe the image information is obtained, which effectively improves the classification and recognition accuracy of liver CT images. The feasibility and effectiveness of the algorithm in this chapter are verified by several comparative experiments, and the features extracted using this algorithm contain both the underlying detail information and the high-level semantic information and thus can adequately characterize the liver CT images.

5. Conclusion

After improving the classical Mumford-Shah model, we give detailed steps of the algorithm, code it, and test it on a 2D medical CT image set. The experiments focus on the segmentation of spleens in CT images. Before the experiments, we train the model with 20 2D images to determine the parameter values of our proposed improved algorithm. In addition, to better analyze the performance of the algorithm, we also performed comparative experiments on the same data using two similar algorithms: the clustering-based image segmentation algorithm and the factorization-based Mumford-Shah model segmentation algorithm. With the results of these experiments, we found that our algorithm has better segmentation results in terms of organs of CT images. In the experiments of segmenting the spleen of CT images, the efficiency and accuracy of our proposed algorithm are better and the segmentation results are better than the other two similar algorithms. In this project, our main object of study is CT images, so we choose a local spectrum histogram for feature extraction, while for other types of image data, other feature extraction algorithms need to be chosen according to the image type and characteristics.

Data Availability

The data used to support the findings of this study are available from the corresponding author upon request.

Conflicts of Interest

The authors declare that they have no known competing financial interests or personal relationships that could have appeared to influence the work reported in this paper.

Acknowledgments

This work was supported by the Shanghai Association of Chinese Integrative Medicine, Scientific Research Fund Project: the Research of Biobank Establishment Standard and Quality Control, No. YG017.

References

[1] A. Onan and S. Korukoğlu, "A feature selection model based on genetic rank aggregation for text sentiment classification," *Journal of Information Science*, vol. 43, no. 1, pp. 25–38, 2017.

[2] B. Durmuş, H. Temurtaş, and S. Özyön, "The design of multiple feedback topology Chebyshev low-pass active filter with average differential evolution algorithm," *Neural Computing and Applications*, vol. 32, no. 22, pp. 17097–17113, 2020.

[3] A. Onan, S. Korukoğlu, and H. Bulut, "A multiobjective weighted voting ensemble classifier based on differential evolution algorithm for text sentiment classification," *Expert Systems with Applications*, vol. 62, pp. 1–16, 2016.

[4] M. Babanezhad, S. Zabihi, I. Behroyan, A. T. Nakhjiri, A. Marjani, and S. Shirazian, "Prediction of gas velocity in two-phase flow using developed fuzzy logic system with differential evolution algorithm," *Scientific Reports*, vol. 11, no. 1, 2021.

[5] Y. Shi, Z. Huo, J. Qin, and Y. Li, "Automatic prior shape selection for image edge detection with modified Mumford-Shah model," *Computers & Mathematics with Applications*, vol. 79, no. 6, pp. 1644–1660, 2020.

[6] S. Lalitha, "An automated lung cancer detection system based on machine learning algorithm," *Journal of Intelligent & Fuzzy Systems*, vol. 40, no. 4, pp. 6355–6364, 2021.

[7] H. Chen and X. Wang, "A deep feature fusion method based on dark channel for medical image segmentation," *Journal of Applied Science and Engineering*, vol. 23, no. 4, pp. 739–745, 2020.

[8] R. Kashyap, "Object boundary detection through robust active contour based method with global information," *International Journal Of Image Mining*, vol. 3, no. 1, pp. 22–37, 2018.

[9] S. M. Ramu, M. Rajappa, K. Krithivasan, and M. R. Nalluri, "A novel fast medical image segmentation scheme for anatomical scans," *Multimedia Tools and Applications*, vol. 78, no. 15, pp. 21391–21422, 2019.

[10] A. Khadidos, V. Sanchez, and C. T. Li, "Weighted level set evolution based on local edge features for medical image segmentation," *IEEE Transactions on Image Processing*, vol. 26, no. 4, pp. 1979–1991, 2017.

[11] J. Verma, M. Nath, P. Tripathi, and K. K. Saini, "Analysis and identification of kidney stone using Kth nearest neighbour (KNN) and support vector machine (SVM) classification techniques," *Pattern Recognition and Image Analysis*, vol. 27, no. 3, pp. 574–580, 2017.

[12] S. Yin, H. Li, D. Liu, and S. Karim, "Active contour modal based on density-oriented BIRCH clustering method for

medical image segmentation," *Multimedia Tools and Applications*, vol. 79, no. 41-42, pp. 31049–31068, 2020.

[13] P. Pachunde, "Efficient automatic segmentation of multi-domain imagery using ensemble feature-segmenter pairs with machine learning," *Turkish Journal of Computer and Mathematics Education (TURCOMAT)*, vol. 12, no. 12, pp. 954–965, 2021.

[14] A. Mihaylova, V. Georgieva, and P. Petrov, "Multistage approach for automatic spleen segmentation in MRI sequences," *International Journal of Reasoning-based Intelligent Systems*, vol. 12, no. 2, pp. 128–137, 2020.

[15] S. Randhawa, A. Alsadoon, P. W. C. Prasad, T. al-Dala'in, A. Dawoud, and A. Alrubaie, "Deep learning for liver tumour classification: enhanced loss function," *Multimedia Tools and Applications*, vol. 80, no. 3, pp. 4729–4750, 2021.

[16] Y. Zhang and L. Niu, "A substructure segmentation method of left heart regions from cardiac CT images using local mesh descriptors, context and spatial location information," *Pattern Recognition and Image Analysis*, vol. 29, no. 2, pp. 230–239, 2019.

[17] H. Ali, S. Faisal, K. Chen, and L. Rada, "Image-selective segmentation model for multi-regions within the object of interest with application to medical disease," *The Visual Computer*, vol. 37, no. 5, pp. 939–955, 2021.

[18] Z. Wang, B. Ma, and Y. Zhu, "Review of level set in image segmentation," *Archives of Computational Methods in Engineering*, vol. 28, no. 4, pp. 2429–2446, 2021.

[19] Q. Huang, Y. Zhou, L. Tao et al., "A Chan-Vese model based on the Markov chain for unsupervised medical image segmentation," *Tsinghua Science and Technology*, vol. 26, no. 6, pp. 833–844, 2021.

[20] M. T. Dehkordi, "An automated method for brain tumor segmentation based on level set," *International Journal of Computer (IJC)*, vol. 30, no. 1, pp. 59–69, 2018.

[21] A. M. Hasan, "A hybrid approach of using particle swarm optimization and volumetric active contour without edge for segmenting brain tumors in MRI scan," *Indonesian Journal of Electrical Engineering and Informatics (IJEEI)*, vol. 6, no. 3, pp. 292–300, 2018.

[22] M. S. al-Huseiny and A. S. Sajit, "Transfer learning with GoogLeNet for detection of lung cancer," *Indonesian Journal of Electrical Engineering and Computer Science*, vol. 22, no. 2, pp. 1078–1086, 2021.

[23] H. Yu, F. He, and Y. Pan, "A novel region-based active contour model via local patch similarity measure for image segmentation," *Multimedia Tools and Applications*, vol. 77, no. 18, pp. 24097–24119, 2018.

[24] A. Biswas, P. Bhattacharya, and S. P. Maity, "A smart system of 3D liver tumour segmentation," *International Journal of Product Development*, vol. 23, no. 2/3, pp. 89–104, 2019.

[25] A. Onan, "An ensemble scheme based on language function analysis and feature engineering for text genre classification," *Journal of Information Science*, vol. 44, no. 1, pp. 28–47, 2018.

[26] M. Alaei, R. Khorsand, and M. Ramezanpour, "An adaptive fault detector strategy for scientific workflow scheduling based on improved differential evolution algorithm in cloud," *Applied Soft Computing*, vol. 99, p. 106895, 2021.